

Registering Source Tokens to Target Language Spaces in Multilingual Neural Machine Translation

Zhi Qu¹ Yiran Wang² Jiannan Mao³

Chenchen Ding^{1,2} Hideki Tanaka² Masao Utiyama² Taro Watanabe¹

¹Nara Institute of Science and Technology, Japan.

{qu.zhi.pv5, taro}@is.naist.jp

²National Institute of Information and Communications Technology, Japan.

{yiran.wang, chenchen.ding, hideki.tanaka, mutiyama}@nict.go.jp

³Gifu University, Japan.

mao@mat.info.gifu-u.ac.jp

Abstract

The multilingual neural machine translation (MNMT) enables arbitrary translations across multiple languages by training a model with limited parameters using parallel data only. However, the performance of such MNMT models still lags behind that of large language models (LLMs), limiting their practicality. In this work, we address this limitation by introducing **registering** to achieve the new state-of-the-art of decoder-only MNMT models. Specifically, we insert a set of artificial tokens specifying the target language, called registers, into the input sequence between the source and target tokens. By modifying the attention mask, the target token generation only pays attention to the activation of registers, representing the source tokens in the target language space. Experiments on EC-40, a large-scale benchmark, show that our method outperforms related methods driven by optimizing multilingual representations. We further scale up and collect 9.3 billion sentence pairs across 24 languages from public datasets to pre-train two models, namely MITRE (**m**ultilingual **t**ranslation with **r**egisters). One of them, MITRE-913M, outperforms NLLB-3.3B, achieves comparable performance with commercial LLMs, and shows strong adaptability in fine-tuning. Finally, we open-source our models to facilitate further research and development in MNMT: <https://github.com/zhiqu2/mitre>.¹

1 Introduction

Multilingual neural machine translation (MNMT) trains models using parallel data to enable translations across multiple languages while maintaining the minimal number of parameters (Firat et al., 2016; Fan et al., 2020; NLLB Team, 2022). MNMT is practically appealing due to its potential for zero-shot translation, i.e., translating language pairs unseen during training, which addresses data scarcity

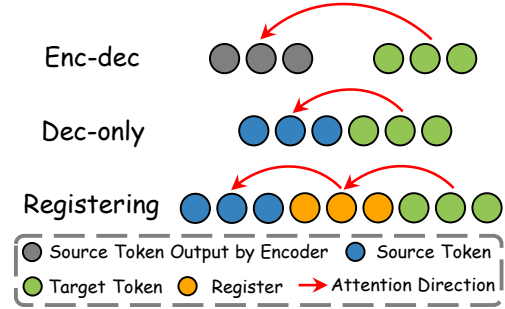


Figure 1: Illustration of the attention view among different architectures. "Token" refers to the representation corresponding to the token.

in certain translation directions (Johnson et al., 2017; Fan et al., 2020; Zhang et al., 2020). However, the usability of MNMT methods remains limited, as their performance lags behind that of large language models (LLMs) (Zhu et al., 2023; Xu et al., 2024). Moreover, zero-shot translation suffers from the off-target problem (Chen et al., 2023; Tan and Monz, 2023), where translations fail to reach the expected target language. This problem is commonly attributed to weak translation instructions, which manifest in two ways: (1) the model ignores translation cues and defaults to a dominant language, such as en² (Qu and Watanabe, 2022); and (2) the generated language becomes entangled with the target language at the representation level (Stap et al., 2023; Qu et al., 2024a). Rather than enhancing translation instructions, we hypothesize that the off-target problem could be resolved by constraining target token generation within the target language space.

We present a novel, simple yet effective method named **registering** to improve MNMT models with the decoder-only architecture (Dec-only) without introducing additional parameters. As illustrated in Figure 1, target token generation pays attention to source tokens in the encoder-decoder (Enc-dec)

¹Partial works done during Zhi Qu's internship at ASTREC of NICT, Japan.

²Languages are denoted by ISO 639-1 codes, https://www.loc.gov/standards/iso639-2/php/code_list.php.

and Dec-only architectures. In registering, the target token generation computes attention for a set of artificial tokens, named **registers**, i.e., a set of instructions for target language matching the length of source tokens, located between source and target tokens in the input sequence by modifying the attention mask. Since registers represent only the target language without carrying semantics with each register aligned with a source token, their activation is expected to mirror the representation of the source tokens in the target language space.

We have conducted two sets of experiments, evaluated with four automatic metrics: spBLEU (NLLB Team, 2022), chrF++ (Popović, 2015, 2017), COMET (Rei et al., 2020), and off-target ratio (Zhang et al., 2020). First, we experiment with EC-40 (Tan and Monz, 2023), an English-centric and large-scale benchmark designed to assess zero-shot translation capability. Experimental results demonstrate that our method improves spBLEU scores by up to 71% on average across 1,640 directions with fewer parameters, substantially outperforming related methods driven by optimizing multilingual representations, and drastically reduces the off-target ratio from 26.69% to 3.65%. In the second set, we collect 9.3 billion sentence pairs across 24 languages by sampling from the NLLB open dataset (NLLB Team, 2022) with the bridge language strategy (Fan et al., 2020). We then pre-train two models, MITRE-466M and MITRE-913M (multilingual translation with registers). MITRE-913M not only surpasses NLLB-3.3B (NLLB Team, 2022) and GPT-3.5 Turbo (Brown et al., 2020) but also achieves competitive performance with GPT-4o mini (OpenAI, 2024). Finally, we fine-tune the pre-trained models in three distinct scenarios, demonstrating the superior adaptability of MITRE in fine-tuning. By analyzing the attention mechanisms in sentence pairs with special syntactic structures and applying dimensionality reduction to token representations sampled from random translation instances, we confirm that the register mirrors the corresponding source token in the target language space.

2 Multilingual Translation With Registers

2.1 Multilingual Neural Machine Translation

Given a multilingual corpus \mathbb{C} spanning multiple translation directions, each instance in \mathbb{C} is defined as (\mathbf{x}, \mathbf{y}) , consisting of a source sentence $\mathbf{x} = x_1, \dots, x_I$ and a target sentence $\mathbf{y} = y_1, \dots, y_J$.

To represent the K languages present in \mathbb{C} , we introduce a set of language tags $\mathbb{L} = \{l_1, \dots, l_K\}$, where each tag is an artificial token corresponding to a language in \mathbb{C} . Following Johnson et al. (2017); Wu et al. (2021), we add a tag indicating the language of \mathbf{y} at the beginning of \mathbf{x} as the translation instruction for multilingual neural machine translation (MNMT), denoted by $l_{\mathbf{y}}$. Consequently, the input fed into the MNMT model becomes $\mathbf{x}' = l_{\mathbf{y}}, x_1, \dots, x_I$. Formally, we train the model over all instances of \mathbb{C} by optimizing the following cross entropy loss:

$$\mathcal{L}_{\text{ce}} = - \sum_{\mathbf{x}', \mathbf{y} \in \mathbb{C}} \sum_{j=1}^J \log p(y_j | \mathbf{x}', \mathbf{y}_{<j}), \quad (1)$$

where $p(y_j | \mathbf{x}', \mathbf{y}_{<j})$ represents the probability distribution for generating y_j by MNMT model. The current state-of-the-art MNMT models (Raffel et al., 2019; Fan et al., 2020; NLLB Team, 2022) utilize the encoder-decoder architecture (Enc-dec), where the generation of y_j can be expressed as:

$$y_j = \text{decoder}(\text{encoder}(\mathbf{x}'), \mathbf{y}_{<j}). \quad (2)$$

Conversely, Gao et al. (2022); Zhang et al. (2022); Qu et al. (2024b) seek to transition the MNMT model to a decoder-only architecture (Dec-only), leveraging the strong zero-shot capabilities inherent to Dec-only models (Wang et al., 2022). In this setup, the generation³ can be described as:

$$y_j = \text{decoder}(\mathbf{x}', \mathbf{y}_{<j}). \quad (3)$$

2.2 Registering

As discussed above, MNMT typically relies on a single language tag, $l_{\mathbf{y}}$, to instruct the translation direction, which is inherently fragile, as the generation of target tokens cannot strictly depend on $l_{\mathbf{y}}$, leading to the risk of off-target problem (Gu et al., 2019; Chen et al., 2023). In this work, we introduce registering to strictly constrain generation within the target language space for a Dec-only model. We begin by initializing a set of artificial tokens corresponding to the target language, denoted by $\mathbf{r} = r_1, \dots, r_{I+1}$, matching the length of \mathbf{x}' . Notably, since the register shares the same target language tag with $l_{\mathbf{y}}$, \mathbf{r} is initialized by duplicating

³Although Dec-only is prevalent in LLMs, training a Dec-only MNMT model applies Equation 1 rather than the language modeling loss (Radford et al., 2018), as Gao et al. (2022) empirically demonstrate that the language modeling loss does not benefit MNMT.

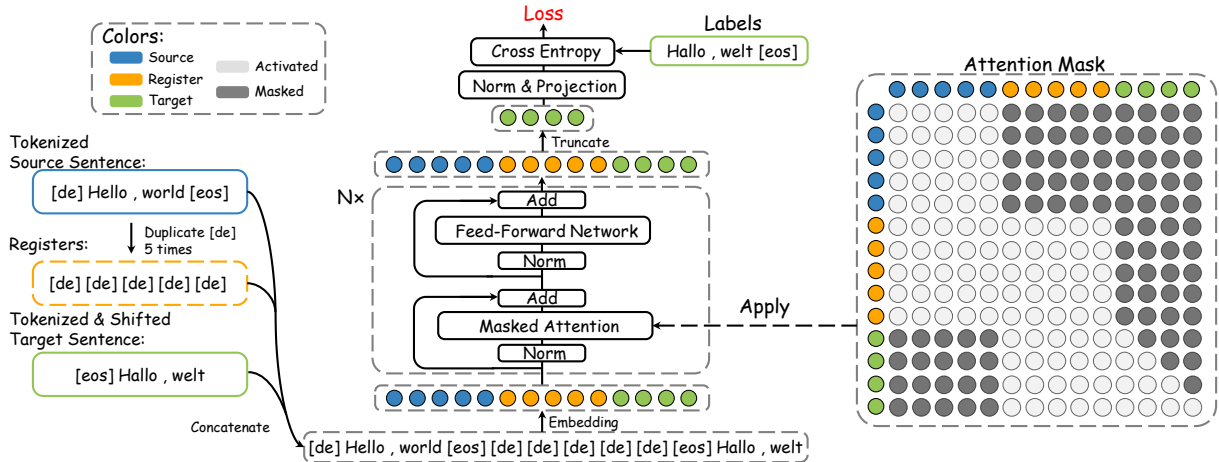


Figure 2: Illustration of registering. The example depicts a translation from en to de. The illustrated model stacks N layers, each following the Transformer decoder layer structure (Vaswani et al., 2017) with pre-normalization (Xiong et al., 2020). Notably, each circle represents a token and its representation in the generation process.

l_y to avoid additional parameters. We then insert r into the input sequence between x' and y , thus reformulating the generation process of Dec-only model as:

$$y_j = \text{decoder}(x', r, y_{<j}). \quad (4)$$

The key step of registering is modifying the Transformer attention mask (Vaswani et al., 2017) to remove source tokens from the view of target tokens. As shown in Figure 2, we initialize the attention mask in the prefix Dec-only style (Dong et al., 2019), where self-attention among source tokens is bi-directional. We then adjust the mask to control token-level representation according to the following rules: (1) x' computes bi-directional attention for x' ; (2) r computes bi-directional attention for x' and r ; (3) y_j pays attention to r and $y_{<j}$. As a result, the generation of y solely relies on the activation of r , namely, the generation is strictly constrained within the target language space to minimize the risk of off-target problems. We think the activation of a register is ideally equivalent to the representation of the positional-aligned source token in the target language space because r functions purely as a structural base for the target language without semantics.

3 Experiment: On Benchmark

3.1 Dataset and Evaluation

We conduct the first set of experiments on EC-40 (Tan and Monz, 2023), which is a large-scale English-centric benchmark designed to evaluate zero-shot translation capabilities. The training data⁴ consists of 120 million sentence pairs span-

ning 41 languages from five language families. Except for English, each family includes eight languages, categorized into four resource tiers, namely, High, Medium, Low, and Extra Low, corresponding to 5 million, 1 million, 100,000, and 50,000 sentence pairs, respectively. The English-centric setup of EC-40 means that all training translation directions involve English, either as the source or target language, resulting in the trained MNMT models supporting 1,640 translation directions. In contrast to the original setup in Tan and Monz (2023), we follow NLLB Team (2022); Cao et al. (2024) to standardize the validation and testing processes using the Flores⁵, which is a high-quality parallel dataset available for over 200 languages. Specifically, we use the Flores *dev* and *devtest* sets for validation and testing, containing 997 and 1,012 sentences per language, respectively.

In the evaluation, we set the beam size to 5 in inference. To compare the performance of our proposed method and related methods, we use four automatic metrics to evaluate inference results on the test set. First, spBLEU (NLLB Team, 2022), a variant of BLEU (Papineni et al., 2002; Post, 2018) used for Flores, unifies tokenization across languages through an open-source tokenizer⁶. Second, chrF++ (Popović, 2015, 2017) assesses character-level overlap and balances precision with recall. Third, COMET⁷ (Rei et al., 2020) evaluates quality by comparing generated translations, reference translations, and source sentences at a representa-

⁵<https://github.com/openlanguagedata/flores>.

⁶<https://tinyurl.com/flores200sacrebleuspm>.

⁷All COMET scores are computed using *Unbabel/wmt22-comet-da* (Rei et al., 2022).

⁴Details of EC-40 are described in Appendix A.

		High		Med		Low		Extra Low						
#params	Method	→	←	→	←	→	←	→	←	sup.	zero.	avg.	off.(%)	
Enc-dec	242M	vanilla	9.46	11.05	7.49	9.80	5.03	3.95	5.41	2.59	29.06	5.86	6.99	48.40
		+CL	14.21	14.19	12.19	14.18	7.89	7.55	7.66	6.04	29.03	9.74	10.68	19.08
		+LCS	10.44	13.67	9.34	13.17	8.73	6.07	8.49	4.10	29.18	8.35	9.37	22.43
Dec-only	217M	vanilla	11.57	11.51	9.48	11.03	6.01	6.06	5.74	4.20	28.61	7.30	8.34	22.21
		+TDO	13.33	13.50	10.53	12.75	7.13	6.88	6.74	4.60	28.84	8.62	9.61	27.18
		+Ours	15.43	15.46	13.88	14.62	8.94	8.99	8.76	7.94	28.90	11.05	11.92	4.65
Enc-dec	418M	vanilla	12.66	15.02	10.86	14.50	7.40	5.04	7.12	3.47	30.28	8.64	9.69	26.69
		+CL	15.89	15.97	13.67	16.15	8.36	8.16	8.32	5.96	30.54	10.79	11.76	19.99
		+LCS	10.79	16.19	10.00	15.31	9.99	5.39	9.41	3.70	30.33	9.25	10.28	23.47
Dec-only	368M	vanilla	14.37	15.07	12.25	15.02	8.27	7.40	7.71	5.11	29.97	9.84	10.82	19.01
		+TDO	15.27	15.79	12.83	15.56	8.44	7.96	8.15	5.40	30.23	10.40	11.37	23.14
		+Ours	16.81	16.98	15.25	16.57	10.10	9.88	9.64	8.37	29.88	12.26	13.12	3.65

Table 1: Averaged spBLEU scores of results on EC-40, the last column (off.) lists the off-target ratio averaged from all directions, the scores of chrF++ and COMET are reported in Tables 7 and 8, as discussed in Appendix H. We report scores by grouping the languages that have the same resource tier. Then, → includes directions translating from the corresponding group to languages out of this group, and ← includes directions translating to the corresponding group. sup., zero, and avg. abbreviate the average of supervised translations, the average of zero-shot translations, and the average of all translations, respectively. The best score in each column of a block is in bold.

tion level. Finally, we report the off-target ratio (Zhang et al., 2020) as a supplementary metric, because the testing tool⁸ is not absolutely accurate as it relies on recognizing language-specific tokens. Since COMET and off-target ratio evaluations lack support for certain languages, we compute these scores only for supported languages, as listed in Appendix G.

3.2 Configuration and Baseline

The modeling follows the manner of Transformer (Vaswani et al., 2017) with an embedding size of 1,024, an inner size of 4,096, and 16 attention heads. We divide the models into two configurations based on model depth. we first stack 12 layers in modeling and balance the number of layers between the encoder and decoder in Enc-dec, resulting in 242M parameters for Enc-dec and 217M parameters for Dec-only. Then, models include 24 layers in the second configuration, yielding 418M parameters for Enc-dec and 368M parameters for Dec-only. We list all training details in Appendix C.

Apart from the vanilla Enc-dec and Dec-only, we reproduce three related methods without additional parameters by the same setting to reflect the effectiveness of registering. (1) CL (Pan et al., 2021): This method aligns sentence-level semantic representations output from the encoder and is included as a baseline since it is the defacto state-of-the-art method. (2) LCS (Sun et al., 2024): LCS follows the translation instruction strategy of Fan

et al. (2020) by adding a source language tag at the beginning of the source tokens and a target language tag at the beginning of the target tokens. LCS then biases the token representations in the encoder by adding the embedding of the target language tag. We include it here as the biasing mechanism of LCS resembles that of r , though it employs a different operation. (3) TDO (Qu et al., 2024b): TDO divides the process of Dec-only into two phases, specifically, encoding source tokens with stronger target language features at the first phase, and then, concatenating the encoded source tokens and target tokens to feed into Dec-only models. We include it as TDO effectively improves the performance of Dec-only MNMT models.

3.3 Result

The results of experiments on EC-40, shown in Table 1, show consistent trends across both configurations. First, our method consistently performs the best. The most notable improvement is in the off-target ratio, where our method reduces this metric from 48.40% to 4.65% in 12-layer models and from 26.69% to 3.65% in 24-layer models. Despite the inaccuracy of the measuring tool, these results indicate that registering nearly resolves the off-target problem. While our method does not achieve the highest performance in supervised translation, it is at the same level as the two Dec-only baselines. Specifically, the higher supervised performance of vanilla models is attributed to the overfitting (Gu et al., 2019; Liu et al., 2021). Then, the similar performance among the three Enc-dec baselines in

⁸<https://github.com/LlmKira/fast-langdetect>.

Family (Group)	Languages	Bridge
English*	en	en
Germanic	de, nl, sv, da, af	de, nl
Romance	fr, es, it, pt, ro	fr, es
Slavic	ru, cs, pl, bg, uk	ru, cs
Malayo-Polynesian	id, ms, jv, tl	id, ms
Asian*	ja, zh, ko, vi	ja, zh

Table 2: Languages in data collection. Decoration with * indicates a language group instead of a language family.

supervised translation supports the observation by Zhang et al. (2022) that the lower supervised performance of Dec-only models compared to Enc-dec models is attributed to the fewer parameters.

We also observe that the gains of spBLEU scores from related methods tend to diminish as model parameters increase. In the 12-layer models, the improvements for CL, LCS, and TDO over vanilla models in translating to High, Med, Low, and Extra Low resource languages are 3.14/3.38/3.60/3.55, 2.62/3.37/2.12/1.51, and 1.99/1.72/0.82/0.40, respectively. In 24-layer models, improvements decrease to 0.95/1.65/3.12/2.49, 1.17/0.81/0.35/0.23, and 0.72/1.06/0.56/0.29, respectively. However, our method achieves more consistent improvements with gains of 3.95/3.59/2.93/3.74 in 12-layer models and 1.91/1.55/2.48/3.26 in 24-layer models. From this comparison, we draw two conclusions: (1) our proposed method, registering, demonstrates superior scalability, and (2) it is highly effective for low-resource languages.

4 Experiment: Pre-trained Models

4.1 Data Collection with Bridge Languages

A robust and practical MNMT model expects training on a dataset supervised across multiple translation directions rather than being English-centric (Zhang et al., 2020; Eriguchi et al., 2022; NLLB Team, 2022). However, collecting data for every possible translation direction is infeasible, as the number of directions grows exponentially with the number of supported languages. In this work, limited by our computational resources, we adopt the Bridge Language strategy (Fan et al., 2020) to collect data across 24 languages spanning more than five language families. Specifically, as shown in Table 2, we group languages by family except for English. The Germanic, Romance, and Slavic groups belong to European language families, and the Malayo-Polynesian differs significantly from these European languages. Additionally, we define a special group, Asian, which includes four

languages predominantly used in the Asian continent: ja, zh, ko, and vi. While these languages belong to different families, they share certain similarities due to their geographic proximity. We designate the two most resource-rich languages in each group as bridge languages and follow these rules for data collection: (1) en connects with all languages; (2) bridge languages connect with each other; (3) bridge languages connect with the remaining languages within their respective groups. Given that ms cannot meet rules (2) and (3) due to its low resource, we collect additional data for ms where possible. Based on the above strategy, out of 552 possible translation directions, we collect data from the reproduced version of the NLLB dataset⁹ (NLLB Team, 2022) for a total of 194 directions, resulting in 9.3 billion sentence pairs for our pre-training.¹⁰

4.2 Configuration and Baseline

We begin by training a vocabulary of 160,000 tokens using SentencePiece (Kudo and Richardson, 2018) on a random sample of 150 million sentences from the training set. We then pre-train two MNMT models, named MITRE (**multilingual translation with registers**), on 80 Tesla V100 GPUs with 466 million and 913 million parameters, respectively. We report the details of modeling and training in Appendix D. The validation and testing process aligns with Section 3.1.

We compare our model against popular and state-of-the-art models. First, the MNMT models include three versions of M2M (483M¹¹, 615M, and 1.2B) (Fan et al., 2020) and three versions of NLLB (615M-distilled, 1.3B, and 3.3B) (NLLB Team, 2022). Also, we include commercial LLMs, GPT-3.5 Turbo¹² (Brown et al., 2020) and GPT-4o mini¹³ (OpenAI, 2024). Meanwhile, we include NLLB-615M and NLLB-1.3B as baselines in our fine-tuning experiments. Specifically, we create three scenarios by randomly selecting 5, 25, and 100 translation directions from the possible directions and perform full-parameter fine-tuning on the Flores *dev*, which contains 997 sentence pairs per direction. Complete training details of fine-tuning are provided in Appendix E.

⁹<https://opus.nlpl.eu/NLLB/corpus/version/NLLB>

¹⁰Appendix B reports the data distribution at the language-family and language level.

¹¹The official name is M2M-418M, however, this model actually has 483M parameters.

¹²Version is *gpt-3.5-turbo-0125*.

¹³Version is *gpt-4o-mini-2024-07-18*.

Model	English		Germanic		Romance		Slavic		Mal.-Polyn.		Asian		avg.	
	→	←	→	←	→	←	→	←	→	←	→	←		
M2M	483M	30.36	31.92	24.40	22.58	24.01	25.81	22.59	23.40	17.94	16.50	18.30	18.37	22.10
	615M	30.69	31.98	26.35	25.56	25.47	27.52	24.02	24.77	20.11	17.49	19.31	19.09	23.65
	1.2B	35.92	35.14	29.51	26.82	28.40	28.38	26.58	26.19	18.09	17.57	15.48	20.07	24.69
NLLB	615M	35.85	41.04	28.13	27.41	27.46	29.09	25.40	25.33	25.39	24.35	20.72	19.42	26.05
	1.3B	38.08	43.42	30.52	30.17	29.63	31.42	27.84	28.25	28.08	26.87	23.50	21.06	28.51
	3.3B	39.80	45.08	31.93	31.77	30.88	32.62	29.29	30.13	29.81	28.08	25.18	22.56	30.01
GPT	3.5 turbo	38.27	42.37	31.01	31.02	30.09	32.73	28.56	27.85	26.75	22.81	23.61	24.08	28.66
	4o mini	41.49	43.97	33.09	31.92	31.40	34.03	30.54	30.69	31.01	27.20	26.34	27.53	31.09
MITRE	466M	40.20	42.60	32.14	31.51	31.32	33.26	29.36	29.80	28.46	26.16	24.05	23.56	29.77
	913M	41.16	44.17	33.34	32.95	32.53	34.23	30.74	31.26	29.90	27.22	25.93	25.58	31.15

Table 3: Averaged spBLEU scores comparing MITRE with baselines. The off-target ratio is not reported due to the near-zero values in these large-scale models. chrF++ and COMET scores are provided in Tables 9 and 10, as discussed in Appendix I. Mal.-Polyn. abbreviates Malayo-Polynesian, and other abbreviations follow Table 1. Prompts used for GPT are reported in Appendix F. Additionally, we use green boxes to highlight scores exceeding NLLB-3.3B and blue boxes for those surpassing GPT-4o Mini, where blue box has the priority.

4.3 Main Results

The experimental results comparing MITRE with baselines are shown in Table 3. We observe that although NLLB-3.3B surpasses MITRE-913M by 0.91 spBLEU scores for translations into English and by 0.86 scores for Malayo-Polynesian languages, MITRE-913M consistently achieves higher scores in other translation directions, with an overall average gain of 1.14 scores. Given that NLLB even surpasses GPT-4o mini by 1.11 scores in English translation, we infer that MITRE, a Dec-only model with registering, demonstrates better generalization than NLLB, based on Enc-dec. Notably, scaling parameters of NLLB from 1.3B to 3.3B yields only a gain of 1.50 scores, while MITRE attains a comparable gain of 1.38 scores with approximately 450M additional parameters. Furthermore, the alignment of training and validation loss for two MITRE models (Appendix D) reinforces our conclusion in Section 3.3 that registering provides superior scalability. Finally, based on all experimental results, we conclude that MITRE-466M performs competitively with NLLB-3.3B, while MITRE-913M not only outperforms NLLB-3.3B but also performs on par with GPT-4 Mini, showing the practical potential of our models.

4.4 Fine-tuning Results

Table 4 shows the fine-tuning results. By comparing NLLB and MITRE, we observe that MITRE outperforms NLLB in both scenarios: fine-tuning on a few translation directions and fine-tuning on multiple directions simultaneously. Notably, the performance gains from fine-tuning increase with model size. Specifically, NLLB-615M achieves spBLEU score improvements of 1.59/1.44/1.33

model		5-direction		25-direction		100-direction	
		spB.	com.	spB.	com.	spB.	com.
N.-615M	pre.	24.00	82.91	25.88	83.71	25.37	83.35
	f.t.	25.59	83.80	27.32	84.29	26.70	84.17
N.-1.3B	pre.	26.59	84.86	28.33	85.41	27.82	85.17
	f.t.	28.50	85.78	30.13	86.09	29.61	86.05
M.-466M	pre.	24.51	83.73	28.71	85.41	29.07	85.26
	f.t.	28.19	85.28	30.61	86.36	30.81	86.45
M.-913M	pre.	25.52	84.56	29.95	86.07	30.37	85.92
	f.t.	30.09	86.45	32.47	87.23	32.73	87.35

Table 4: Averaged spBLEU and COMET scores of results on three fine-tuning scenarios, where the specific translation directions are listed in Appendix B. N., M., pre., and f.t. abbreviate NLLB, MITRE, pre-trained model, and fine-tuned model, respectively. The best score is in bold, blue boxes highlights the largest gain in f.t. relative to pre., and green boxes highlights the second-largest.

in the three scenarios, while NLLB-1.3B shows gains of 1.91/1.80/1.79. MITRE-466M achieves improvements of 3.68/1.90/1.74, whereas MITRE-913M shows gains of 4.57/2.52/2.36. Additionally, given that pre-trained models of both NLLB and MITRE achieve near-zero off-target ratios, those gains are attributed to the increased quality instead of improving the off-target problem, suggesting that MITRE has a higher performance ceiling, likely due to our cost-saving data collection strategy, which may have constrained MITRE from reaching its theoretical maximum. Therefore, given the superior fine-tuning capability of MITRE, we argue the practical potential of MITRE again.

5 Discussion

5.1 Ablation Study

We conduct two ablation studies to measure the impact of registering. First, we decompose registering into two steps: (1) adding registers and (2)

#layer	register	mask	spB. \uparrow	chr \uparrow	com. \uparrow	off. \downarrow
12	✗	✗	8.34	22.34	55.71	22.21
	✓	✗	8.19	22.96	55.72	32.11
	✓	✓	11.92	29.02	61.19	4.65
24	✗	✗	10.82	26.04	59.95	19.01
	✓	✗	8.91	24.06	57.60	34.22
	✓	✓	13.12	30.51	63.54	3.65

Table 5: Averaged scores of ablation study on EC-40. Here, register means adding registers, and mask means modifying the attention mask.

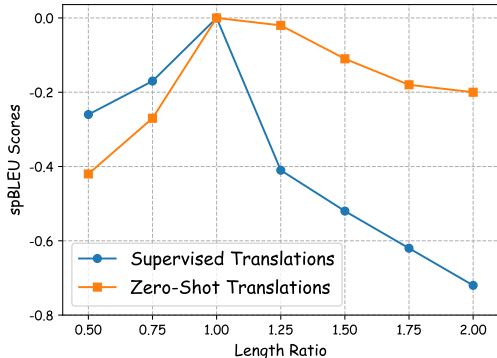


Figure 3: The spBLEU score variations on EC-40 with different length ratios of r to x' , where only the length of r is changed and x' is fixed.

modifying the attention mask. As shown in Table 5, merely adding registers reduces the performance of vanilla Dec-only models; registering only becomes effective after modifying the attention mask. This result aligns with expectations, i.e., the model without constraints on generation defaults to relying directly on source tokens instead of registers.

In Section 2.2, we introduce that the lengths of r and x are matched to ensure a one-to-one correspondence between registers and source tokens. To validate this design, we vary the length of r while keeping x' fixed to observe performance trends. Specifically, a ratio less than 1.0 means that r augments x' , while a ratio greater than 1.0 means r compresses x' . The trend illustrated in Figure 3, where the length ratio of 1.0 is the optimal case, empirically supports our design.

5.2 Mechanism of Registering

We analyze multilingual representations and attention weights to explore the registering mechanism and validate our design. First, we analyze token representations by randomly selecting 100 translation instances from three translation directions and applying t-SNE (van der Maaten and Hinton, 2008) to reduce them to two dimensions, as shown in Figure 4. In the final model layer, we observe

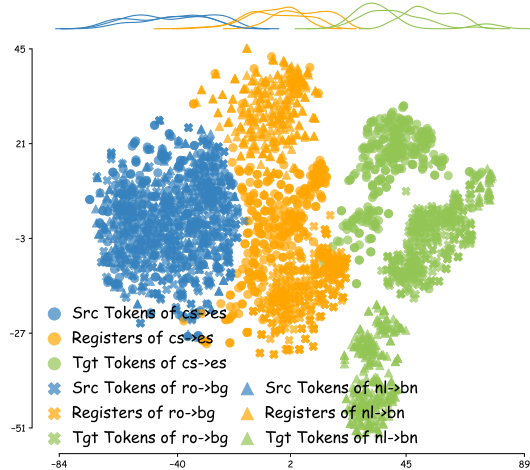


Figure 4: 2D distribution of token-level representations extracted from the output of the 24th layer of a model trained on EC-40. Each class listed in the legend contains 300 randomly sampled tokens. Appendix K shows the representational distributions from other layers.

that source tokens, registers, and target tokens are clearly separated into distinct spaces, indicating that registers successfully remove source tokens from the view of target tokens at the representation level. Additionally, source token representations from different languages cluster together, suggesting that the model processes them in a language-agnostic status. Most importantly, registers and target tokens are grouped into different spaces corresponding to the target language.

We further examine the attention weights of our models by using two translation instances from de to en, where the source sentence involves the special grammatical structure of de, i.e., separable verb. As shown in Figure 5, although those two different source sentences of de are translated into the same target sentence, the simple verb, i.e., “öffne”, shown in Figure 5a semantically equals to the separable verb not forming a constituent, i.e., “mache ... auf”, shown in Figure 5b. As a result, we observe that each register consistently places its highest attention on its positionally-aligned source token, followed by contextual attention to related tokens. Then, in Figure 5a, r_1 has strong attention to both “öffne” and “Tür”, while both r_1 and r_6 pay attention to “mache ... auf” and “Tür” in Figure 5b. Furthermore, we find that the attention of target tokens to registers aligns with the structure of the source sentence. Specifically, in Figure 5a, “open” primarily has attention to r_1 , whereas “open” pays attention to both r_1 and r_6 in Figure 5b. Additionally, other tokens in both instances follow the pattern that each register represents the same se-

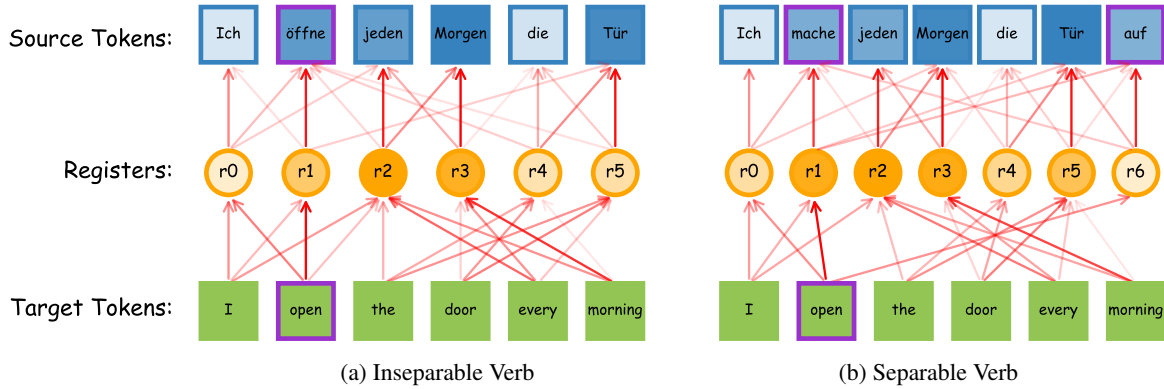


Figure 5: Attention weights averaged across all layers of a model trained on EC-40. These two instances, both translating from de to en, share the same semantics and translate to the same target sentence. Although two verbs in source sentences exhibit different forms, they are semantically equivalent, where verbs are highlighted in purple. The top-3 attention directions for each token are labeled, with darker colors indicating higher attention weights.

mantics as the corresponding source token.¹⁴ Combined with the representational clusters, we conclude that the mechanism of registering aligns with our design, namely, the activation of registers is equivalent to the representation of source tokens within the target language space.

6 Related Work

Three works are methodologically related to ours. [Mu et al. \(2023\)](#) propose a method, called gisting, which involves appending a set of gist tokens after prompts in LLMs and modifying the attention mask so that these tokens consistently correspond to a given prompt. During inference, only the gist tokens are used, eliminating the need for the original prompts. [Darcet et al. \(2024\)](#) introduce a method for Vision Transformers by adding a set of artificial tokens to the input, also termed registers. However, their registers function solely as dummy placeholders without participating in generation. Additionally, registering also can be regarded as an implicit chain-of-thought ([Wei et al., 2023](#)), where the process serves as "rethinking" the source tokens from the perspective of the target language.

In MNMT, we successfully migrate the architecture of MNMT models from the standard encoder-decoder paradigm ([Raffel et al., 2019](#); [Fan et al., 2020](#); [NLLB Team, 2022](#)) to a decoder-only structure, building on the efforts of [Zhang et al. \(2022\)](#); [Gao et al. \(2022\)](#); [Caillaut et al. \(2024\)](#). Our method combines two primary research directions: (1) making source tokens language-agnostic to enhance zero-shot translation ([Pan et al., 2021](#); [Gu and Feng, 2022](#); [Gao et al., 2023](#); [Bu et al., 2024](#)),

and (2) strengthening target language information to improve the generation process ([Kudugunta et al., 2019](#); [Stap et al., 2023](#); [Qu et al., 2024a](#)). Similar to our motivation, [Chen et al. \(2023\)](#) constrain the generation of target tokens by target-language-specific vocabulary. Notably, [Lu et al. \(2018\)](#); [Zhu et al. \(2020\)](#) also explicitly introduce an intermediate state to support the target token generation, whereas their design aims to get a language-agnostic state, which is contrary to our design, i.e., registering source tokens into the target language space. Additionally, given that the performance of MNMT models often lags behind that of LLMs, [Yang et al. \(2023\)](#); [Xu et al. \(2024\)](#) focus on fine-tuning LLMs for MNMT-specific models. However, we show that developing MNMT with parallel data only remains a promising prospect.

7 Conclusion

In this work, we present registering to achieve state-of-the-art performance in multilingual neural machine translation (MNMT). By introducing registers and modifying the attention mask, our method ensures that the generation of target tokens depends solely on the activation of registers rather than on source tokens. Analysis experiments demonstrate that the activation of registers is equivalent to the representation of source tokens within the target language spaces. Using this method, we develop and open-source two pre-trained models, MITRE-466M and MITRE-913M, supporting translation across 24 languages. Experimental results show that MITRE not only surpasses previous MNMT models but also performs competitively with commercial LLMs, setting a new state-of-the-art in multilingual translation.

¹⁴We show more examples in Appendix J.

8 Limitation

A key concern is our limited computational resources. Given that the training of MITRE-913M has already required 80 Tesla V100 GPUs for one month, MITRE supports 24 languages and we cannot further increase the supported languages. Although this number is far greater than the latest research in the community, e.g., 10 languages of [Alves et al. \(2024\)](#) and 5 languages of [Xu et al. \(2024\)](#), this number is fewer than supported languages of M2M, NLLB, and commercial LLMs. However, the comparison in Section 4 is relatively fair. Specifically (using NLLB as an example), first, our training data is collected from the reproduced version of the NLLB dataset, which includes fewer samples per translation direction than those used in training NLLB models. Second, as described in Section 4.1, our Bridge Language strategy results in fewer supervised translation directions, whereas NLLB is trained on as many directions as possible. Moreover, NLLB incorporates additional engineering strategies, e.g., back-translation ([Edunov et al., 2018](#)) and distillation ([Hinton et al., 2015](#)), whereas MITRE only iterates over the training set. Also, we directly compare MITRE-466M and MITRE-913M with NLLB-3.3B, where the parameter size difference helps offset the disparity in supported languages. Finally, we conduct fine-tuning experiments to compare MITRE and NLLB with the same settings.

Another limitation of our approach is the additional computational cost introduced by registers, as they double the number of source tokens. Based on our measurements on EC-40 using a Tesla V100 GPU, the training time for models with registers is 1.34 times that of the vanilla decoder-only model, 1.63 times that of the vanilla encoder-decoder model, and approximately equivalent (1.01 times) to the previous state-of-the-art method, CL ([Pan et al., 2021](#)). During inference, thanks to the KV Cache (refer to incremental decoding in Fairseq), the model with registers merely incurs a 1.1 times increase in computational cost compared to the vanilla decoder-only model. However, in practical usage, i.e., MITRE, the cost time of inference is substantially lower than that of NLLB and LLMs due to the smaller number of parameters.

9 Ethical Consideration

Although our training data is collected from public datasets, MITRE has not been evaluated for toxicity

or undergone detoxification. Thus, while we open-source MITRE, we recommend its use primarily for research purposes or in applications only after thorough appropriate processing.

References

- Duarte M. Alves, José Pombal, Nuno M. Guerreiro, Pedro H. Martins, João Alves, Amin Farajian, Ben Peters, Ricardo Rei, Patrick Fernandes, Sweta Agrawal, Pierre Colombo, José G. C. de Souza, and André F. T. Martins. 2024. [Tower: An open multilingual large language model for translation-related tasks](#). *Preprint*, arXiv:2402.17733.
- Naveen Arivazhagan, Ankur Bapna, Orhan Firat, Dmitry Lepikhin, Melvin Johnson, Maxim Krikun, Mia Xu Chen, Yuan Cao, George Foster, Colin Cherry, Wolfgang Macherey, Zhifeng Chen, and Yonghui Wu. 2019. [Massively multilingual neural machine translation in the wild: Findings and challenges](#). *Preprint*, arXiv:1907.05019.
- Tom B. Brown, Benjamin Mann, Nick Ryder, Melanie Subbiah, Jared Kaplan, Prafulla Dhariwal, Arvind Neelakantan, Pranav Shyam, Girish Sastry, Amanda Askell, Sandhini Agarwal, Ariel Herbert-Voss, Gretchen Krueger, Tom Henighan, Rewon Child, Aditya Ramesh, Daniel M. Ziegler, Jeffrey Wu, Clemens Winter, Christopher Hesse, Mark Chen, Eric Sigler, Mateusz Litwin, Scott Gray, Benjamin Chess, Jack Clark, Christopher Berner, Sam McCandlish, Alec Radford, Ilya Sutskever, and Dario Amodei. 2020. [Language models are few-shot learners](#). *Preprint*, arXiv:2005.14165.
- Mengyu Bu, Shuhao Gu, and Yang Feng. 2024. [Improving multilingual neural machine translation by utilizing semantic and linguistic features](#). In *Findings of the Association for Computational Linguistics ACL 2024*, pages 10410–10423, Bangkok, Thailand and virtual meeting. Association for Computational Linguistics.
- Gaëtan Caillaut, Raheel Qader, Mariam Nakhlé, Jingshu Liu, and Jean-Gabriel Barthélemy. 2024. [Scaling laws of decoder-only models on the multilingual machine translation task](#). *Preprint*, arXiv:2409.15051.
- Zhe Cao, Zhi Qu, Hidetaka Kamigaito, and Taro Watanabe. 2024. [Exploring intrinsic language-specific subspaces in fine-tuning multilingual neural machine translation](#). *Preprint*, arXiv:2409.05224.
- Liang Chen, Shuming Ma, Dongdong Zhang, Furu Wei, and Baobao Chang. 2023. [On the off-target problem of zero-shot multilingual neural machine translation](#). In *Findings of the Association for Computational Linguistics: ACL 2023*, pages 9542–9558, Toronto, Canada. Association for Computational Linguistics.
- Timothée Darcet, Maxime Oquab, Julien Mairal, and Piotr Bojanowski. 2024. [Vision transformers need](#)

- registers. In *The Twelfth International Conference on Learning Representations*.
- Li Dong, Nan Yang, Wenhui Wang, Furu Wei, Xiaodong Liu, Yu Wang, Jianfeng Gao, Ming Zhou, and Hsiao-Wuen Hon. 2019. [Unified language model pre-training for natural language understanding and generation](#). *Preprint*, arXiv:1905.03197.
- Sergey Edunov, Myle Ott, Michael Auli, and David Grangier. 2018. [Understanding back-translation at scale](#). In *Proceedings of the 2018 Conference on Empirical Methods in Natural Language Processing*, pages 489–500, Brussels, Belgium. Association for Computational Linguistics.
- Akiko Eriguchi, Shufang Xie, Tao Qin, and Hany Hassan Awadalla. 2022. [Building multilingual machine translation systems that serve arbitrary x-y translations](#). *Preprint*, arXiv:2206.14982.
- Angela Fan, Shruti Bhosale, Holger Schwenk, Zhiyi Ma, Ahmed El-Kishky, Siddharth Goyal, Mandeep Baines, Onur Celebi, Guillaume Wenzek, Vishrav Chaudhary, Naman Goyal, Tom Birch, Vitaliy Liptchinsky, Sergey Edunov, Edouard Grave, Michael Auli, and Armand Joulin. 2020. [Beyond english-centric multilingual machine translation](#). *Preprint*, arXiv:2010.11125.
- Orhan Firat, Baskaran Sankaran, Yaser Al-onaizan, Fatos T. Yarman Vural, and Kyunghyun Cho. 2016. [Zero-resource translation with multi-lingual neural machine translation](#). In *Proceedings of the 2016 Conference on Empirical Methods in Natural Language Processing*, pages 268–277, Austin, Texas. Association for Computational Linguistics.
- Pengzhi Gao, Liwen Zhang, Zhongjun He, Hua Wu, and Haifeng Wang. 2023. [Improving zero-shot multilingual neural machine translation by leveraging cross-lingual consistency regularization](#). In *Findings of the Association for Computational Linguistics: ACL 2023*, pages 12103–12119, Toronto, Canada. Association for Computational Linguistics.
- Yingbo Gao, Christian Herold, Zijian Yang, and Hermann Ney. 2022. [Is encoder-decoder redundant for neural machine translation?](#) In *Proceedings of the 2nd Conference of the Asia-Pacific Chapter of the Association for Computational Linguistics and the 12th International Joint Conference on Natural Language Processing (Volume 1: Long Papers)*, pages 562–574, Online only. Association for Computational Linguistics.
- Jiatao Gu, Yong Wang, Kyunghyun Cho, and Victor O.K. Li. 2019. [Improved zero-shot neural machine translation via ignoring spurious correlations](#). In *Proceedings of the 57th Annual Meeting of the Association for Computational Linguistics*, pages 1258–1268, Florence, Italy. Association for Computational Linguistics.
- Shuhao Gu and Yang Feng. 2022. [Improving zero-shot multilingual translation with universal representations and cross-mapping](#). In *Findings of the Association for Computational Linguistics: EMNLP 2022*, pages 6492–6504, Abu Dhabi, United Arab Emirates. Association for Computational Linguistics.
- Geoffrey Hinton, Oriol Vinyals, and Jeff Dean. 2015. [Distilling the knowledge in a neural network](#). *Preprint*, arXiv:1503.02531.
- Melvin Johnson, Mike Schuster, Quoc V. Le, Maxim Krikun, Yonghui Wu, Zhifeng Chen, Nikhil Thorat, Fernanda Viégas, Martin Wattenberg, Greg Corrado, Macduff Hughes, and Jeffrey Dean. 2017. [Google’s multilingual neural machine translation system: Enabling zero-shot translation](#). *Transactions of the Association for Computational Linguistics*, 5:339–351.
- Diederik P. Kingma and Jimmy Ba. 2017. [Adam: A method for stochastic optimization](#). *Preprint*, arXiv:1412.6980.
- Taku Kudo and John Richardson. 2018. [SentencePiece: A simple and language independent subword tokenizer and detokenizer for neural text processing](#). In *Proceedings of the 2018 Conference on Empirical Methods in Natural Language Processing: System Demonstrations*, pages 66–71, Brussels, Belgium. Association for Computational Linguistics.
- Sneha Kudugunta, Ankur Bapna, Isaac Caswell, and Orhan Firat. 2019. [Investigating multilingual NMT representations at scale](#). In *Proceedings of the 2019 Conference on Empirical Methods in Natural Language Processing and the 9th International Joint Conference on Natural Language Processing (EMNLP-IJCNLP)*, pages 1565–1575, Hong Kong, China. Association for Computational Linguistics.
- Danni Liu, Jan Niehues, James Cross, Francisco Guzmán, and Xian Li. 2021. [Improving zero-shot translation by disentangling positional information](#). In *Proceedings of the 59th Annual Meeting of the Association for Computational Linguistics and the 11th International Joint Conference on Natural Language Processing (Volume 1: Long Papers)*, pages 1259–1273, Online. Association for Computational Linguistics.
- Yichao Lu, Phillip Keung, Faisal Ladhak, Vikas Bhardwaj, Shaonan Zhang, and Jason Sun. 2018. [A neural interlingua for multilingual machine translation](#). In *Proceedings of the Third Conference on Machine Translation: Research Papers*, pages 84–92, Brussels, Belgium. Association for Computational Linguistics.
- Jesse Mu, Xiang Lisa Li, and Noah Goodman. 2023. [Learning to compress prompts with gist tokens](#). In *Thirty-seventh Conference on Neural Information Processing Systems*.
- NLLB Team. 2022. [No language left behind: Scaling human-centered machine translation](#). *Preprint*, arXiv:2207.04672.

- OpenAI. 2024. [Gpt-4 technical report](#). *Preprint*, arXiv:2303.08774.
- Myle Ott, Sergey Edunov, Alexei Baevski, Angela Fan, Sam Gross, Nathan Ng, David Grangier, and Michael Auli. 2019. [fairseq: A fast, extensible toolkit for sequence modeling](#). In *Proceedings of the 2019 Conference of the North American Chapter of the Association for Computational Linguistics (Demonstrations)*, pages 48–53, Minneapolis, Minnesota. Association for Computational Linguistics.
- Xiao Pan, Mingxuan Wang, Liwei Wu, and Lei Li. 2021. [Contrastive learning for many-to-many multilingual neural machine translation](#). In *Proceedings of the 59th Annual Meeting of the Association for Computational Linguistics and the 11th International Joint Conference on Natural Language Processing (Volume 1: Long Papers)*, pages 244–258, Online. Association for Computational Linguistics.
- Kishore Papineni, Salim Roukos, Todd Ward, and Wei-Jing Zhu. 2002. [Bleu: a method for automatic evaluation of machine translation](#). In *Proceedings of the 40th Annual Meeting of the Association for Computational Linguistics*, pages 311–318, Philadelphia, Pennsylvania, USA. Association for Computational Linguistics.
- Maja Popović. 2015. [chrF: character n-gram F-score for automatic MT evaluation](#). In *Proceedings of the Tenth Workshop on Statistical Machine Translation*, pages 392–395, Lisbon, Portugal. Association for Computational Linguistics.
- Maja Popović. 2017. [chrF++: words helping character n-grams](#). In *Proceedings of the Second Conference on Machine Translation*, pages 612–618, Copenhagen, Denmark. Association for Computational Linguistics.
- Matt Post. 2018. [A call for clarity in reporting BLEU scores](#). In *Proceedings of the Third Conference on Machine Translation: Research Papers*, pages 186–191, Brussels, Belgium. Association for Computational Linguistics.
- Zhi Qu, Chenchen Ding, and Taro Watanabe. 2024a. [Languages transferred within the encoder: On representation transfer in zero-shot multilingual translation](#). *Preprint*, arXiv:2406.08092.
- Zhi Qu, Yiran Wang, Chenchen Ding, Hideki Tanaka, Masao Utiyama, and Taro Watanabe. 2024b. [Improving language transfer capability of decoder-only architecture in multilingual neural machine translation](#). *Preprint*, arXiv:2412.02101.
- Zhi Qu and Taro Watanabe. 2022. [Adapting to non-centered languages for zero-shot multilingual translation](#). In *Proceedings of the 29th International Conference on Computational Linguistics*, pages 5251–5265, Gyeongju, Republic of Korea. International Committee on Computational Linguistics.
- Alec Radford, Karthik Narasimhan, Tim Salimans, Ilya Sutskever, et al. 2018. [Improving language understanding by generative pre-training](#).
- Colin Raffel, Noam Shazeer, Adam Roberts, Katherine Lee, Sharan Narang, Michael Matena, Yanqi Zhou, Wei Li, and Peter J. Liu. 2019. [Exploring the limits of transfer learning with a unified text-to-text transformer](#). *Preprint*, arXiv:1910.10683.
- Ricardo Rei, José G. C. de Souza, Duarte Alves, Chrysoula Zerva, Ana C Farinha, Taisiya Glushkova, Alon Lavie, Luisa Coheur, and André F. T. Martins. 2022. [COMET-22: Unbabel-IST 2022 submission for the metrics shared task](#). In *Proceedings of the Seventh Conference on Machine Translation (WMT)*, pages 578–585, Abu Dhabi, United Arab Emirates (Hybrid). Association for Computational Linguistics.
- Ricardo Rei, Craig Stewart, Ana C Farinha, and Alon Lavie. 2020. [COMET: A neural framework for MT evaluation](#). In *Proceedings of the 2020 Conference on Empirical Methods in Natural Language Processing (EMNLP)*, pages 2685–2702, Online. Association for Computational Linguistics.
- David Stap, Vlad Niculae, and Christof Monz. 2023. [Viewing knowledge transfer in multilingual machine translation through a representational lens](#). In *Findings of the Association for Computational Linguistics: EMNLP 2023*, pages 14973–14987, Singapore. Association for Computational Linguistics.
- Zengkui Sun, Yijin Liu, Fandong Meng, Jinan Xu, Yufeng Chen, and Jie Zhou. 2024. [LCS: A language converter strategy for zero-shot neural machine translation](#). In *Findings of the Association for Computational Linguistics ACL 2024*, pages 9201–9214, Bangkok, Thailand and virtual meeting. Association for Computational Linguistics.
- Shaomu Tan and Christof Monz. 2023. [Towards a better understanding of variations in zero-shot neural machine translation performance](#). In *Proceedings of the 2023 Conference on Empirical Methods in Natural Language Processing*, pages 13553–13568, Singapore. Association for Computational Linguistics.
- Laurens van der Maaten and Geoffrey Hinton. 2008. [Visualizing data using t-sne](#). *Journal of Machine Learning Research*, 9(86):2579–2605.
- Ashish Vaswani, Noam Shazeer, Niki Parmar, Jakob Uszkoreit, Llion Jones, Aidan N Gomez, Łukasz Kaiser, and Illia Polosukhin. 2017. [Attention is all you need](#). In *Advances in Neural Information Processing Systems*, volume 30. Curran Associates, Inc.
- Thomas Wang, Adam Roberts, Daniel Hesslow, Teven Le Scao, Hyung Won Chung, Iz Beltagy, Julien Launay, and Colin Raffel. 2022. [What language model architecture and pretraining objective work best for zero-shot generalization?](#) *Preprint*, arXiv:2204.05832.

Jason Wei, Xuezhi Wang, Dale Schuurmans, Maarten Bosma, Brian Ichter, Fei Xia, Ed Chi, Quoc Le, and Denny Zhou. 2023. [Chain-of-thought prompting elicits reasoning in large language models](#). *Preprint*, arXiv:2201.11903.

Liwei Wu, Shanbo Cheng, Mingxuan Wang, and Lei Li. 2021. [Language tags matter for zero-shot neural machine translation](#). In *Findings of the Association for Computational Linguistics: ACL-IJCNLP 2021*, pages 3001–3007, Online. Association for Computational Linguistics.

Ruibin Xiong, Yunchang Yang, Di He, Kai Zheng, Shuxin Zheng, Chen Xing, Huishuai Zhang, Yanyan Lan, Liwei Wang, and Tie-Yan Liu. 2020. [On layer normalization in the transformer architecture](#). *Preprint*, arXiv:2002.04745.

Haoran Xu, Young Jin Kim, Amr Sharaf, and Hany Hassan Awadalla. 2024. [A paradigm shift in machine translation: Boosting translation performance of large language models](#). In *The Twelfth International Conference on Learning Representations*.

Wen Yang, Chong Li, Jiajun Zhang, and Chengqing Zong. 2023. [Bigtranslate: Augmenting large language models with multilingual translation capability over 100 languages](#). *Preprint*, arXiv:2305.18098.

Biao Zhang, Behrooz Ghorbani, Ankur Bapna, Yong Cheng, Xavier Garcia, Jonathan Shen, and Orhan Firat. 2022. [Examining scaling and transfer of language model architectures for machine translation](#). In *Proceedings of the 39th International Conference on Machine Learning*, volume 162 of *Proceedings of Machine Learning Research*, pages 26176–26192. PMLR.

Biao Zhang, Philip Williams, Ivan Titov, and Rico Senrich. 2020. [Improving massively multilingual neural machine translation and zero-shot translation](#). In *Proceedings of the 58th Annual Meeting of the Association for Computational Linguistics*, pages 1628–1639, Online. Association for Computational Linguistics.

Changfeng Zhu, Heng Yu, Shanbo Cheng, and Weihua Luo. 2020. [Language-aware interlingua for multilingual neural machine translation](#). In *Proceedings of the 58th Annual Meeting of the Association for Computational Linguistics*, pages 1650–1655, Online. Association for Computational Linguistics.

Wenhao Zhu, Hongyi Liu, Qingxiu Dong, Jingjing Xu, Shujian Huang, Lingpeng Kong, Jiajun Chen, and Lei Li. 2023. [Multilingual machine translation with large language models: Empirical results and analysis](#). *Preprint*, arXiv:2304.04675.

A Description of EC-40

EC-40 is an English-centric dataset introduced by [Tan and Monz \(2023\)](#). In addition to English, it includes 40 languages spanning five language

Family	ISO code	Flores code	Language	script
Germanic	en	eng_Latn	English	Latin
	de	deu_Latn	German	Latin
	nl	nld_Latn	Dutch	Latin
	sv	swe_Latn	Swedish	Latin
	da	dan_Latn	Danish	Latin
	af	afr_Latn	Afrikaans	Latin
Romance	fr	fra_Latn	French	Latin
	es	spa_Latn	Spanish	Latin
	it	ita_Latn	Italian	Latin
	pt	por_Latn	Portuguese	Latin
	ro	ron_Latn	Romanian	Latin
Slavic	ru	rus_Cyrl	Russian	Cyrillic
	cs	ces_Latn	Czech	Latin
	pl	pol_Latn	Polish	Latin
	bg	bul_Cyrl	Bulgarian	Cyrillic
	uk	ukr_Cyrl	Ukrainian	Cyrillic
Malayo-Polynesian	id	ind_Latn	Indonesian	Latin
	ms	zsm_Latn	Malay	Latin
	jv	jav_Latn	Javanese	Latin
	tl	fil_Latn	Filipino	Latin
Asian*	ko	kor_Hang	Korean	Hangul
	vi	vie_Latn	Vietnamese	Latin
	ja	jpn_Jpan	Japanese	Kanji; Kana
	zh	cmn_Hans	Chinese	Chinese

Table 6: Details of the dataset in our pre-training. The decoration * on Asian means a group instead of a language family. We not only list the ISO 639-1 code for each language but also list the Flores code to help search corresponding resources from Flores+.

families, with each family containing eight languages. These languages are categorized into four tiers based on data availability: High, Medium, Low, and Extra Low. Each non-English language is paired with English, resulting in 80 supervised translation directions used for training and 1,560 zero-shot translation directions. Details of this dataset are summarized in Table 11.

B Description of Pre-training Dataset

Our pre-training dataset comprises 24 languages, as detailed in Table 6. As described in Section 4.1, our data collection strategy results in 9.3 billion translation instances across 194 translation directions. The data distribution is visualized at the family level in Figure 8a and at the language level in Figure 8b. Additionally, Figure 8b highlights which translation directions are supervised and which are zero-shot. Notably, translation directions involving ms are also indicated in Figure 8b.

C Training Details of EC-40

Training configurations We employ Fairseq ([Ott et al., 2019](#)), an open-source toolkit, to implement our models with methods mentioned in

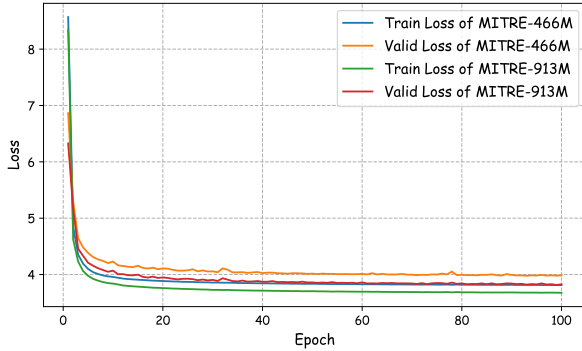


Figure 6: The training and validation loss in pre-training MITRE. We report the first 100 epochs, each with approximately 2262 steps.

Section 3.2. First, we directly reuse the vocabulary and binary training data provided by Chen et al. (2023)¹⁵. Note that we include only supervised translation directions in validation. We train on 8 Tesla V100 GPUs, setting *memory-efficient-fp16* in Fairseq, with a maximum input of 2048 source tokens per GPU and a gradient accumulation of 16 steps. Both input and output token lengths are limited to 256, and we share the embedding layer between the encoder and decoder. We use a seed of 1234, a learning rate of 0.0005 with the inverse square root schedule and a warmup of 4000 steps, the Adam optimizer (Kingma and Ba, 2017), dropout of 0.1, attention dropout of 0.1, a label smoothing rate of 0.1, no weight decay, and the temperature sampling with $T = 5$ (Arivazhagan et al., 2019). Finally, we train for 200,000 steps, averaging the last 5 checkpoints, saving by epoch.

Configurations of Related Methods For CL (Pan et al., 2021), we directly reuse their code¹⁶ and set the contrastive learning temperature to 0.1, which is the optimal setting according to their reports. For LCS (Sun et al., 2024), we reimplement their code and, in the case of 12-layer models where the encoder has 6 layers, apply LCS biasing at the 5th encoder layer; For models with 12 encoder layers, we apply it at the 8th encoder layer. For TDO (Qu et al., 2024b), we also reuse their code and, based on their ablation study, set the number of layers for the first stage to 3 in 12-layer models and to 6 in 24-layer models to allow stronger zero-shot translation ability.

D Training Details of MITRE

We employ Fairseq to implement MITRE mentioned in Section 4.2, and two versions of MITRE have the different configurations in modeling and have the same configuration in training. Specifically, MITRE-466M is configured with an embedding size of 1,024, an inner size of 4,096, 16 attention heads, and 24 layers. MITRE-913M, a larger model with expanded width and depth, has an embedding size of 1,280, an inner size of 5,120, 20 heads, and 36 layers. In training, we first train a shared SentencePiece vocabulary (Kudo and Richardson, 2018) with a size of 160,000 by 150 million sentences randomly sampled from the training set. We include only supervised translation directions in validation. Then, we train on 80 Tesla V100 GPUs, setting *memory-efficient-fp16* in Fairseq, with a maximum input of 1408 source tokens per GPU and a gradient accumulation of 10 steps. In practice, this setup results in each batch containing approximately 0.91 million source tokens. Given the large batch size, we set the learning rate of 0.002 with the inverse square root schedule and the warmup of 8000 steps. We also use a seed of 42, the Adam optimizer (Kingma and Ba, 2017), dropout of 0.1, attention dropout of 0.1, a label smoothing rate of 0.1, no weight decay, and the temperature sampling with $T = 1$ (Arivazhagan et al., 2019). We train for 300,000 steps and save a checkpoint per 10,000 steps. Finally, we average the last 5 checkpoints. Figure 6 shows the variations of training and validation loss. We can observe that the trends of MITRE-466M and MITRE-913M are highly consistent.

E Training Details of Fine-tuning

Selecting Directions We use *random.sample* in Python to randomly select translation directions for fine-tuning, setting the seed to 0. We define three scenarios, including 5, 25, and 100 translation directions. It is important to note that *random.sample* causes the 5 and 25 directions to be subsets of the 100 directions. Specifically, the first 5 and first 25 directions in the 100-direction set correspond to the other two scenarios. The 100 directions are: $jk \rightarrow sv$, $ms \rightarrow id$, $de \rightarrow tl$, $ru \rightarrow pl$, $ko \rightarrow jv$, $zh \rightarrow bg$, $ms \rightarrow en$, $pl \rightarrow ru$, $zh \rightarrow af$, $uk \rightarrow ko$, $pt \rightarrow jv$, $ko \rightarrow ro$, $fr \rightarrow da$, $cs \rightarrow pl$, $fr \rightarrow af$, $da \rightarrow fr$, $ru \rightarrow sv$, $fr \rightarrow pl$, $pl \rightarrow tl$, $da \rightarrow ro$, $sv \rightarrow es$, $bg \rightarrow jv$, $zh \rightarrow en$, $da \rightarrow cs$,

¹⁵<https://github.com/Smu-Tan/ZS-NMT-Variations>

¹⁶<https://github.com/PANxiao1994/mRASP2>

uk→ms, tl→es, bg→de, pt→nl, vi→bg, tl→id, ru→bg, nl→ms, en→uk, da→sv, jv→ms, en→nl, zh→vi, bg→ja, ro→ja, bg→ru, nl→tl, vi→es, ja→pt, cs→uk, da→ko, af→it, jv→zh, zh→cs, sv→da, ko→pt, cs→nl, pt→vi, nl→en, vi→ja, es→nl, tl→ru, ru→es, ja→jv, ro→zh, nl→ro, fr→jv, cs→fr, fr→cs, uk→jv, ko→bg, cs→da, es→ro, ms→sv, ja→cs, cs→en, da→pl, jv→tl, pl→pt, zh→sv, pl→de, fr→ro, pt→zh, zh→id, pl→fr, ko→ru, it→bg, es→de, cs→tl, af→pt, fr→ru, da→nl, da→af, ms→fr, ko→cs, en→jv, pl→uk, bg→uk, af→tl, ro→bg, de→pl, de→vi, uk→nl, id→ja, nl→zh, zh→pl

Fine-tuning Configurations All fine-tuning experiments use the same settings. We conduct experiments on 8 Tesla V100 GPUs, with a maximum of 1024 tokens per GPU and a gradient accumulation of 2 steps. Based on the pre-trained model, we set the learning rate to 0.0001 with a warmup step of 1 (for launching the inverse square root schedule), and train for 10 epochs. Finally, we use the last epoch for testing.

F Prompts for GPT

Our prompts for GPT series follow: Translating the following sentence from [SRC] to [TGT]: [INPUT]. Here, [SRC] and [TGT] are the source and target language names following Table 6, and [INPUT] is the source sentence. We find that GPT occasionally repeats [INPUT] in the output. Once it happens, we manually remove the [INPUT] before evaluation.

G Details of Evaluation Metrics

In evaluating the performance of models trained on EC-40, some languages lack support from COMET (*Unbabel/wmt22-comet-da*) and the off-target ratio (*fast-langdetect*). Notably, *fast-langdetect* operates by word recognition, so we also exclude certain supported languages that exhibit low recognition success rates. We list the supported languages in this section.

Languages in COMET: en, bg, so, ca, da, be, bs, es, uk, am, hi, ro, no, de, cs, pt, nl, mr, is, ne, ur, ha, sv, gu, ar, fr, ru, it, pl, sr, sd, he, af, kn, bn.

Languages in Off-target Ratio: en, bg, da, es, uk, hi, ro, de, cs, pt, nl, mr, ur, sv, gu, ar, fr, ru, it, pl, he, kn, bn, be, mt, am, is, sd.

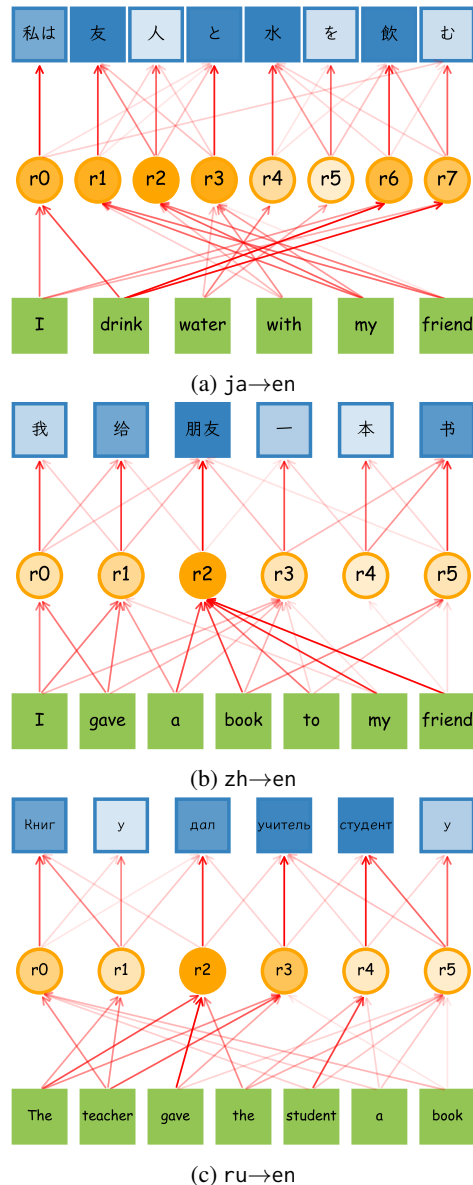


Figure 7: Three cases of attention analysis on MITRE-466M. Details of this illustration, e.g. colors, classes, and arrows, follow that of Figure 5.

H Supplementary Results of EC-40

In Section 3.3 and Table 1, we report spBLEU scores and off-target ratio. In this appendix, we report chrF++ and COMET scores in Tables 7 and 8, respectively. Overall, four metrics show consistent trends across this benchmark.

I Supplementary Results of MITRE

In Section 4.3 and Table 3, we report spBLEU scores and do not report the off-target ratio, because the values are near zero across those large-scale pre-trained models. In this appendix, we report chrF++ and COMET scores in Tables 9 and 10,

respectively. However, contrary to the statement in Appendix H, some differences in performance trends are observed. Overall, MITRE performs relatively better on chrF++ compared to spBLEU but slightly worse on COMET. First, chrF++ essentially acts as a lower bound for spBLEU, as languages not included in the vocabulary are tokenized at the character level. Additionally, based on benchmark results (Section 3.3), registering effectively constrains the representation to the output language, leading MITRE to perform better in sequence-based evaluation metrics. On the other side, since COMET primarily focuses on semantic alignment, it is expected that models with more parameters and more training data might have greater semantic knowledge. Nonetheless, we consider the possibility that even if MITRE’s output aligns closely with the reference, it may be suboptimal for the COMET model in capturing the source sentence’s semantics. This phenomenon warrants further investigation, as it may impact the fairness of COMET evaluations to some extent.

J Supplementary Analysis of Attention

To further support our analysis in Section 5.2, we examine additional cases in MITRE-466M where the source and target sentences exhibit significant structural differences. In all cases, the attention relationship between registers and source tokens remains consistent, i.e., one-to-one attention weights being the most prominent. Next, we observe the following patterns: (1) As shown in Figure 7a, in Japanese, the attention for “drink” points to r_6 , while “friend” points to r_1 and r_2 . (2) As shown in Figure 7b, “friend” points to r_2 , and “book” points to r_5 . (3) As shown in Figure 7c, “book” points to r_0 , and “student” points to r_4 . Given that the attention weights between registers and target tokens highlight the structural differences between source and target sentences, we can state again that registers mirror the corresponding source tokens.

K Supplementary Analysis of Representation

We present Figure 9 to supplement the analysis in Section 5.2 on representation distributions, where Figure 4 focuses specifically on the representation state in the 24th layer. Our observations are as follows: (1) In the embedding layer and the 1st layer output (Figures 9a and 9b), source and target token representations are loosely distributed,

while registers form three compact clusters based on language. This is because registers lack semantic content and are distinguished only by positional encoding. (2) Starting from the 6th layer (Figure 9c), source tokens begin to become distinguishable by language, and registers start to shift within the representation space toward the source tokens. By the 12th layer (Figure 9d), registers and source tokens are entirely separated in the representation space. (3) By the 18th layer (Figure 9e), target tokens become clearly separated in the representation space, registers’ distribution becomes more diffuse, and the distribution of source tokens becomes more concentrated. These trends culminate in the state observed in the 24th layer (Figure 9f), as described in Section 5.2. These findings suggest two key phenomena: (1) registers progressively reinforce the semantic information they carry as they propagate through the layers; and (2) the representations of target tokens reflect their predicted state only in the higher layers.

		High		Med		Low		Extra Low					
#params	Method	→	←	→	←	→	←	→	←	sup.	zero.	avg.	
Enc-dec	242M	vanilla	23.27	25.61	20.43	24.61	16.39	14.25	17.73	13.34	49.27	18.16	19.68
		+CL	31.64	30.87	28.65	31.27	21.38	21.66	21.46	19.33	49.20	24.86	26.04
		+LCS	25.34	31.05	24.13	30.90	24.81	19.84	24.77	17.45	49.34	23.70	24.95
Dec-only	217M	vanilla	27.26	27.10	24.42	27.16	18.30	18.01	18.46	16.17	48.44	21.00	22.34
		+TDO	30.25	29.87	25.87	29.61	20.61	19.75	20.50	18.00	48.92	23.32	24.57
		+Ours	33.74	33.55	31.77	32.47	24.87	24.50	24.82	24.68	48.87	28.00	29.02
Enc-dec	418M	vanilla	27.91	31.84	25.40	31.48	20.57	16.02	20.79	15.33	50.11	22.60	23.95
		+CL	33.02	32.52	29.85	32.84	20.99	22.05	21.84	18.30	50.41	25.51	26.73
		+LCS	24.67	33.81	23.88	32.99	26.30	18.10	25.71	16.87	50.16	24.26	25.57
Dec-only	368M	vanilla	31.01	31.96	28.04	32.20	22.05	20.13	22.02	18.84	49.76	24.82	26.04
		+TDO	32.12	32.22	28.43	32.24	21.84	20.85	22.25	19.32	50.04	25.23	26.44
		+Ours	35.24	35.00	33.31	34.56	26.41	26.01	26.22	25.61	49.69	29.53	30.51

Table 7: Averaged chrF++ scores of results on EC-40. All notations and abbreviations follow Table 1.

		High		Med		Low		Extra Low					
#params	Method	→	←	→	←	→	←	→	←	sup.	zero.	avg.	
Enc-dec	242M	vanilla	50.21	49.61	42.07	44.93	28.62	28.15	32.94	31.17	77.26	52.29	53.72
		+CL	55.33	52.42	46.33	47.60	30.00	31.42	34.17	34.40	77.33	56.75	57.93
		+LCS	50.27	52.22	43.19	47.73	31.88	30.19	37.09	32.50	77.52	55.44	56.71
Dec-only	217M	vanilla	52.66	50.88	43.80	45.88	29.19	30.13	33.88	32.64	77.10	54.41	55.71
		+TDO	54.39	52.48	45.22	47.40	30.09	30.76	34.53	33.59	77.13	56.16	57.36
		+Ours	56.94	54.87	48.74	49.59	32.61	33.83	37.10	37.11	77.12	60.23	61.19
Enc-dec	418M	vanilla	54.06	54.76	45.71	49.32	31.11	29.68	35.37	32.49	78.48	56.84	58.08
		+CL	58.06	55.20	48.40	49.96	30.79	32.53	35.50	35.06	78.90	59.26	60.38
		+LCS	51.52	55.63	44.84	50.74	33.84	30.80	38.91	33.94	78.62	57.61	58.81
Dec-only	368M	vanilla	56.46	55.29	47.26	50.07	31.66	31.85	36.27	34.44	78.37	58.84	59.95
		+TDO	57.49	55.44	48.34	50.48	31.77	32.57	36.61	35.72	78.48	59.77	60.84
		+Ours	58.98	56.92	50.66	51.82	33.91	35.37	38.60	38.04	78.12	62.66	63.54

Table 8: Averaged COMET scores of results on EC-40. All notations and abbreviations follow Table 1.

		English		Germanic		Romance		Slavic		Mal.-Polyn.		Asian		
Model		→	←	→	←	→	←	→	←	→	←	→	←	avg.
M2M	483M	50.43	54.36	44.84	46.24	43.96	48.26	43.36	43.06	37.54	41.77	39.83	27.85	42.53
	615M	49.97	54.74	46.77	48.62	45.34	49.83	44.70	44.42	40.17	43.59	41.04	28.84	44.12
	1.2B	54.80	54.44	49.02	47.06	47.49	48.04	45.87	43.35	32.78	40.68	30.90	28.01	42.56
NLLB	615M	55.54	61.73	48.48	50.39	47.38	51.54	46.38	45.34	45.98	50.96	42.56	29.73	46.70
	1.3B	56.82	63.35	50.07	52.21	48.80	53.19	47.98	47.46	47.92	52.49	44.70	30.98	48.40
	3.3B	57.88	64.27	50.95	53.16	49.63	53.92	48.91	48.76	49.06	53.28	45.71	31.97	49.35
GPT	3.5 turbo	55.30	61.60	49.39	52.16	48.31	53.34	47.54	46.35	45.64	48.05	43.46	31.20	47.41
	4o mini	58.03	62.85	51.26	52.90	49.33	54.33	49.12	48.62	49.39	52.25	45.86	34.11	49.48
MITRE	466M	58.11	62.77	51.40	53.41	50.06	54.46	49.18	48.62	47.83	52.04	45.10	32.41	49.29
	913M	58.84	64.01	52.40	54.59	51.03	55.36	50.32	49.84	48.97	52.88	46.65	33.88	50.42

Table 9: Averaged chrF++ scores of results for comparing MITRE and baselines. All notations and abbreviations follow Table 3.

		English		Germanic		Romance		Slavic		Mal.-Polyn.		Asian		
Model		→	←	→	←	→	←	→	←	→	←	→	←	avg.
M2M	483M	81.63	81.40	78.90	77.03	80.48	78.49	79.85	80.31	68.34	72.75	78.67	78.57	77.74
	615M	81.16	82.15	81.42	79.98	82.00	80.50	81.29	82.43	72.56	74.62	80.02	79.96	79.79
	1.2B	85.93	85.17	84.15	82.87	84.46	83.12	83.87	85.41	75.91	77.83	82.95	82.58	82.66
NLLB	615M	86.61	86.76	84.06	82.77	84.50	83.05	83.41	84.39	81.26	83.51	82.12	82.02	83.33
	1.3B	87.76	87.63	85.72	84.76	85.93	84.76	85.07	86.82	83.57	84.93	84.36	83.52	85.13
	3.3B	88.22	88.09	86.49	85.58	86.58	85.45	85.84	87.96	84.63	85.45	85.42	84.56	85.96
GPT	3.5 turbo	87.67	88.02	86.26	85.80	86.62	85.96	85.91	87.50	83.09	82.09	85.45	85.77	85.66
	4o mini	89.59	88.64	87.50	86.38	87.58	86.57	87.08	88.90	85.89	86.03	86.99	87.47	87.16
MITRE	466M	87.87	87.29	85.99	84.98	86.49	85.14	85.58	87.19	82.24	83.41	84.38	84.29	85.19
	913M	88.11	87.81	86.54	85.61	86.96	85.70	86.16	88.03	83.15	83.80	85.52	85.35	85.88

Table 10: Averaged COMET scores of results for comparing MITRE and baselines. All notations and abbreviations follow Table 3.

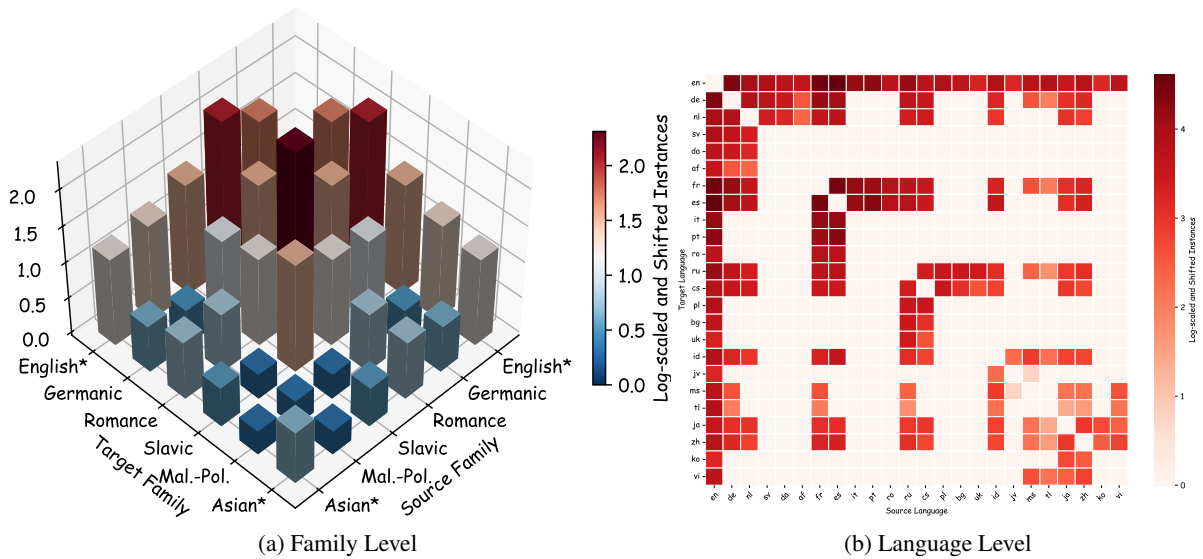


Figure 8: Data distribution of our pre-training dataset. Figure 8a shows data size distribution at the family level, while Figure 8b displays data size at the language level. In 8a, non-zero values are scaled by \log_{10} and adjusted by subtracting 7 for clearer visualization. In 8b, non-zero values are also scaled by \log_{10} and shifted by subtracting the minimum value to enhance illustration clarity.

	Germanic			Romance			Slavic			Indo-Aryan			Afro-Asiatic		
	code	Language	Script	code	Language	Script	code	Language	Script	code	Language	Script	code	Language	Script
High (5 million)	de	German	Latin	fr	French	Latin	ru	Russian	Cyrillic	hi	Hindi	Devanagari	ar	Arabic	Arabic
	nl	Dutch	Latin	es	Spanish	Latin	cs	Czech	Latin	bn	Bengali	Bengali	he	Hebrew	Hebrew
Med (1 million)	sv	Swedish	Latin	it	Italian	Latin	pl	Polish	Latin	kn	Kannada	Devanagari	mt	Maltese	Latin
	da	Danish	Latin	pt	Portuguese	Latin	bg	Bulgarian	Cyrillic	mr	Marathi	Devanagari	ha	Hausa*	Latin
Low (100 thousand)	af	Afrikaans	Latin	ro	Romanian	Latin	uk	Ukrainian	Cyrillic	sd	Sindhi	Arabic	ti	Tigrinya	Ethiopic
	lb	Luxembourgish	Latin	oc	Occitan	Latin	sr	Serbian	Latin	gu	Gujarati	Devanagari	am	Amharic	Ethiopic
Extra Low (50 thousand)	no	Norwegian	Latin	ast	Asturian	Latin	be	Belarusian	Cyrillic	ne	Nepali	Devanagari	kab	Kabyle*	Latin
	ic	Icelandic	Latin	ca	Catalan	Latin	bs	Bosnian	Latin	ur	Urdu	Arabic	so	Somali	Latin

Table 11: Details of non-English languages in EC-40. This table is duplicated from Tan and Monz (2023). Numbers in the table represent the number of sentences paired to the English. Two exceptions are Hausa and Kabyle, where their data sizes are 334,000 and 18,448, respectively.



Figure 9: 2D distributions of token-level representations extracted from the different layers of a model trained on EC-40. This illustration complements Figure 4.